Effect of strain and surface proximity on the acceptor grouping in ZnO

O. Volnianska, V. Ivanov, L. Wachnicki and E. Guziewicz

Institute of Physics, Polish Academy of Sciences

Introduction and DFT methods

The experimentally observed two types of photoelectron spectra (PES) of different crystallites in ZnO and ZnO:N indicate the grouping of acceptor and donor complexes in separate domains [1]:

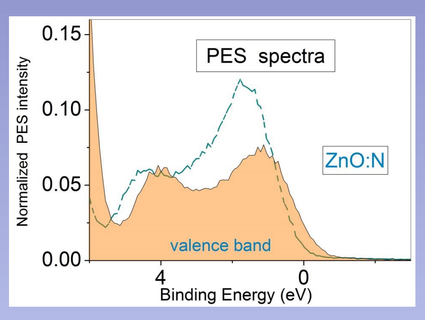

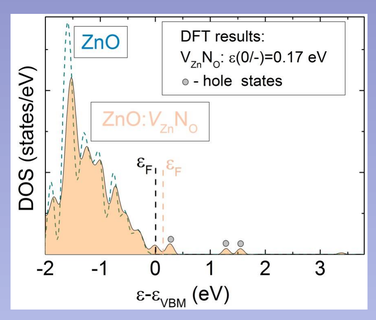

Fig. 1 Normalized PES (a) and (b) calculated Density of states (DOS) of pure ZnO and complexes in ZnO:N. Adapted from Ref. [1]. $V_{Zn}N_O$ – shallow acceptor state, 0/- = 0.17 eV.

Density Functional Theory (DFT) studies suggest that the acceptor domains can involve zinc vacancy (V_{Zn}) and -H_x or -$(NH_x)_O$ groups [1].
$V_{Zn}N_O$ – shallow acceptor state, 0/- = 0.17 eV level above the VBM, but formation energy is high, > 6 eV.
$V_{Zn}N_OH_x$ – formation energies are lower (<3.5 eV) , but these are deep acceptors, for example $V_{Zn}N_OH$ 0/- = 0.9 eV [1, 2-4].
The acceptor-related sample properties depend on a number of factors such as growth or annealing conditions [6]. The introduction of $V_{Zn}N_OH_x$ might provide the first step towards p-type doping before annealing. Both experiments and DFT calculations suggest that at the annealing temperature of 800^{0}C and above the $V_{Zn}N_OH_x$ complex starts to dissociate, to $V_{Zn}N_O$ with hydrogen exiting the sample [1,5].

Both, the formation and dissociation of defects involve distortion of the crystal lattice, so it may be assumed that strain/micro-strain plays an important role here for both defect aggregation and its electronic structure. DFT study of the effect of strain and surface proximity on the formation of (V_{Zn}) -(NHx)O complexes was performed using QUANTUM-ESPRESSO package [6, 7] within the generalized gradient approximation (GGA) with the Hubbard-like +U term describing the on-site Coulomb interactions (U_{zn} =10 eV, U_O = U_N =7 eV). The formation of complexes require the migration of the constituent defects, which was computed using the Nudged Elastic Band (NBE) approach under (a) tensile and compressive biaxial strains in planar plane and uniaxial strain along z-axis, (b) hydrostatic pressure, and (c) local lattice distortion provoked by uncontrolled impurities as CHx groups. Finally , we analyzed surface proximity on the electronic structure and formation energy. In the last case, defects were introduced into the quantum dot (QD) ZnO [8].

Results

A. NEB calculations without strain

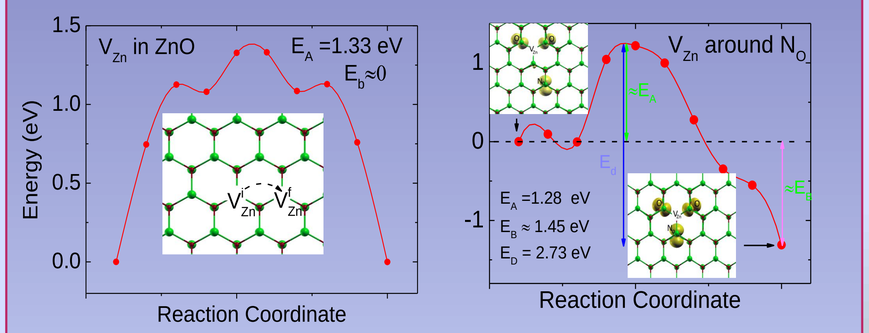

Fig. 2 The calculated NEB paths for migration of neutral zinc vacancy in the pure ZnO (a), in the presence N_O (b), and $(NH)_O$ (c) in N-doped ZnO, and migration of H^+ around $V_{Zn}N_O$. Atomic geometries and spin density distributions of initial and final configurations are presented in insets.

Here, E_A is the migration barrier , E_B is approximated binding energy calculated as $E_B = [E_{form}(A) + E_{form}(B)] - E_{form}(AB)$, where E_{form} (A) or (B) – formation energy of isolated defects, E_{form} (AB) – formation energy of the AB complex. $E_D \approx E_B$(complex) + E_A is associated with the dissociation energy of the complex.

$E_D(V_{Zn}N_O + H^+) < E_D(NH_O + V_{Zn})$, and $E_D(V_{Zn}N_O + H^+)$ is about 0.95 eV which is lower than $E_D(V_{Zn} + N_O)$, so the $V_{Zn}N_O$ pair starts to dissolve at temperatures of about 150^{0}C higher than in the case of $V_{Zn}N_O + H^+$.

B. Defect electronic structure and NEB calculations in strain conditions

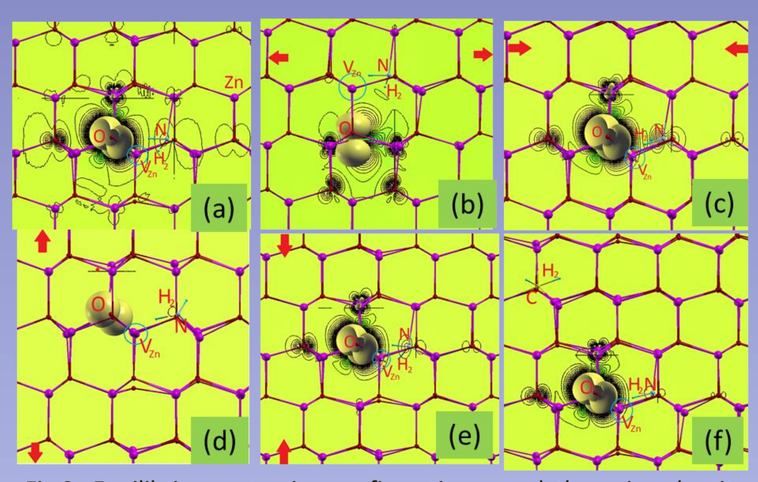

Fig.3. Equilibrium atomic configurations and the spin density isosurface of the $V_{Zn}N_OH_2$ complex: (a) without strain, (b), (c) 4 % tensile and compressive biaxial strain in planar plane, respectively. (d), (e) 4 % tensile and compressive uniaxial strain along z-axis, respectively, (f) in presence of CH_2 as substitution to O atom.

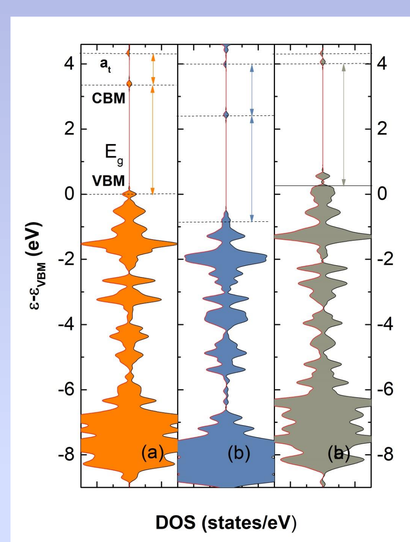

Fig. 4 The total DOS of $V_{Zn}N_OH_2$ (a) without strain, (b), (c) 4 % tensile and compressive biaxial stress in planar plane, respectively.
$V_{Zn}N_OH_2$: the single hole at the three-fold-degenerated t_2 state induces a strong Jahn-Teller effect, which drives a nuclear reorganization and splits $t_{2\downarrow}$ into an occupied $e_{t\downarrow}$ and an empty $a_{t\downarrow}$. The highest horizontal line corresponds to the $a_{t\downarrow}$. VBM and CBM are depicted as horizontal lines. It can be seen that electronic structure is affected by strain asserted along biaxial planar plane .

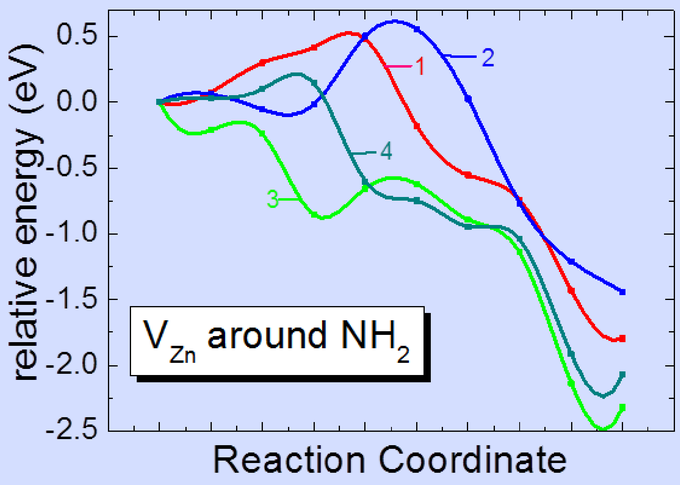

Fig. 5 Reaction paths from NEB calculations for the Zn vacancy around $(NH_2)_O$ at four different strain configurations: 1 – without strain; 2, 3 – 4 % tensile and compressive biaxial strain in planar plan, respectively; 4 – 4 % compressive axial strain along z – axis

Both the migration barrier energy and binding energy dependent on the strain conditions. In particular, 4% compressive biaxial strain along z-axis reduces migration barrier of zinc vacancy moving around (NH_2) from 0.49 eV to 0.25 eV, and 4% compressive strain in xy-plane lead s to the lowering of the migration energy to zero.

References

[1] E. Guziewicz, et al., Phys. Rev. Appl. 18, 044021.
[2] L. Liu, et al., Phys. Rev. Lett. 108, 215501 (2012).
[3] J. Reynolds, et al. , Appl. Phys. Lett. 102, 152114 (2013).
[4] M. Amini et al., Phys. Chem. Chem. Phys. 17, 5485 (2015).
[5] S. Mishra, et al., Phys. Status Solidi A, 2200466 (2022).
[6] P. Giannozzi, et al., J. Phys.: Condens. Matter. 21, 395502 (2009).
[7] M. Cococcioni, S. de Gironcoli, Phys. Rev. B 71, 035105 (2005).
[8] O. Volnianska, J. Chem. Phys. 154, 124710 (2021).

Acknowledgments

The work was supported by the project No. 2018/31/B/ST3/03576, founded by the National Science Centre. Calculations were done at Interdisciplinary Center for Mathematical and Computational Modeling, University of Warsaw .

C. Surface strain

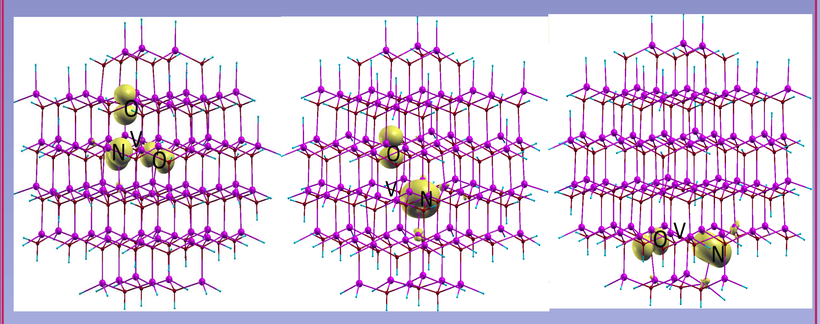

Fig.6. Equilibrium atomic configurations and the spin density isosurface of the $V_{Zn}N_O$ complex at different geometry in respect to the QD center. Three holes in the complex states are located on sp^3(O) and sp^3(N) dangling bonds, but surface proximity affects the shape and the spin structure.

D. Comparison with experiment

Undoped ZnO films, ~100 nm thick, were grown at 300^{o}C by Atomic Layer Deposition (ALD) using diethylzinc and deionized water precursors. Films, deposited on *c*-Al_2O_3 and *a*-Al_2O_3 substrates, were grown in the same ALD process. XRD patterns show that, although the growth process is not epitaxial, the crystallography of the films strongly depends on the substrate orientation.

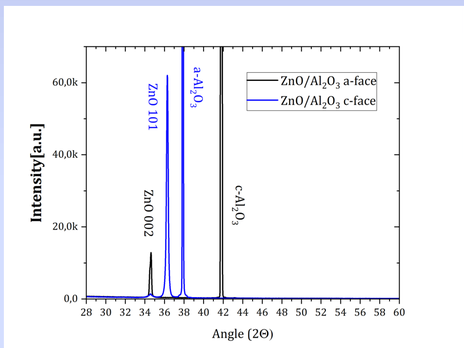

Lattice constant c
ZnO/*a*-Al_2O_3 → 5.18 Å
ZnO/*c*-Al_2O_3 → 5.19 Å

ZnO single crystal
c → 5.2071 Å

Fig. 7. The ZnO/*a*-Al_2O_3 and ZnO/*c*-Al_2O_3 films show 101 and 002 orientations, respectively. The value of strain inside the ZnO/*a*-Al_2O_3 film is higher.

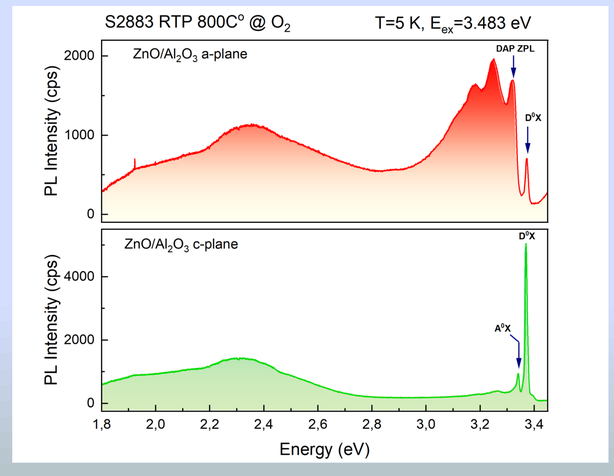

Fig. 8. Photoluminescence spectra measured for ZnO/*a*-Al_2O_3 and ZnO/*c*-Al_2O_3 films show a significant difference in the PL response in the band-edge region. For the ZnO/*a*-Al_2O_3 sample acceptor-related optical transitions are much stronger.

Conclusions

In summary, we show DFT results of systematical analysis of the impact of different strain conditions on the electronic structure and acceptor aggregation for complexes that involve zinc vacancy (V_{Zn}) and -Hx or -$(NHx)_O$ groups. According to the present knowledge, these complexes are responsible for acceptor conductivity of ZnO and ZnO:N.
A wide range of strain conditions were considered: (a) tensile and compressive biaxial strains in planar plane and uniaxial along the z-axis, (b) hydrostatic pressure, and (c) local lattice distortion provoked by uncontrolled impurities as the CHx groups, (d) surface proximity.

The effect of strain explains lowering of acceptor formation energy and might be also responsible for grouping of acceptors which can be formed only in crystallites showing compressive strain or near the surface.

In support to the DFT results, the PL spectra reveal considerably more intensive acceptor luminescence for the samples with higher strain along the c axis.